GEOLOGICA CARPATHICA, DECEMBER 2006, 57, 6, 447–460

Chemical composition of spinels from Mesozoic alkali basalts of the Western Carpathians: implications for sources of detrital spinels in flysch sediments

TOMÁŠ MIKUŠ[1], JÁN SPIŠIAK[1], MILAN SÝKORA[2] and RASTISLAV DEMKO[3]

[1]Geological Institute Slovak Academy of Sciences, Severná 5, 974 01 Banská Bystrica, Slovak Republic; mikus@savbb.sk; spisiak@savbb.sk
[2]Faculty of Natural Sciences, Comenius University, Mlynská dolina, 842 15 Bratislava, Slovak Republic; sykora@fns.uniba.sk
[3]Geological Survey of Slovak Republic, Kynceľovská 10, 974 01 Banská Bystrica, Slovak Republic; demko@gssrbb.sk

(Manuscript received October 16, 2004; accepted in revised form October 5, 2006)

Abstract: Cr-spinel is a relatively widespread accessory heavy mineral in Mesozoic alkali volcanic rocks in the Central Western Carpathians. According to their chemical composition, spinels from these rocks (basalts, submarine hyaloclastites) can be divided into several groups (volcanic — Cr-spinel and Fe-Ti spinel, and peridotitic spinel, altered). Volcanic spinels crystallized in the plumbing system, and peridotitic spinels ultimately originated from peridotitic xenoliths, entrapped and brought to the surface by magmas. Melt/silicate inclusions (clinopyroxenes, plagioclases, melt) were found only in Cr-spinels of volcanic origin. Alteration processes are similar in all studied samples (enrichment in Ti^{4+}, Fe^{2+}, Fe^{3+} and depletion in Mg^{2+} and Al^{3+}). The chemical composition of Cr-spinels from Cretaceous alkali basalts from the Western Carpathians is different to those of detrital Cr-spinels of volcanic origin from the Albian Poruba Flysch Formation. Mesozoic alkali volcanites were not important source for widespread detrital spinels of volcanic origin in Cretaceous sediments (mainly in the Tatric and Fatric Tectonic Units).

Key words: Cretaceous volcanism, Cr-spinel, silicate melt inclusions, clinopyroxene, alteration.

Introduction

Spinel is an important accessory mineral of Mesozoic alkali volcanic rocks because it is resistant to mechanical breakdown and low-grade alteration. Mantle peridotite- and volcanic rock-derived spinels are indicative of magmatic and tectonic evolution and spinel chemistry is diagnostic of melt composition, crystallization conditions and tectonic setting. Although Cretaceous basaltic volcanites were studied mainly from the geochemical point of view in many previous works (e.g. Hovorka & Spišiak 1988; Spišiak & Hovorka 1997; Hovorka et al. 1999), no attention was paid to the chemical composition of spinels. Therefore, we analysed spinels from these rocks in order to obtain information about their petrogenetic nature. With the use of discrimination criteria for spinel compositional variations (Lenaz et al. 2000; Kamenetsky et al. 2001) genetically different spinel types were distinguished. Melt inclusions entrapped within Cr-spinels and clinopyroxene phenocrysts were used to decipher the geochemical character of Cretaceous basaltic rocks of the Central Western Carpathians (CWC). Clinopyroxene inclusions in Cr-spinel were used for thermobarometric calculations. Parental melt composition was recalculated from the association of daughter phases and residual silicic glass composition of melt inclusions entrapped in Cr-spinel.

Many authors have been looking for the source area of a rather widespread detrital Cr-spinel occurring in Cretaceous flysch sediments (e.g. Mišík et al. 1980; Jablonský et al. 2001). For this reason, we considered Cretaceous basalts as a potential important source of flysch-hosted detrital spinel. Thus we compared the composition of spinels from Cretaceous basaltic volcanites with that of detrital spinels from siliciclastic flysch sediments of the Tatric and Fatric Tectonic Units.

Geology and tectonic settings

Mesozoic (Lower Cretaceous) alkali rocks of various types occur in the External (EWC) and Central Western Carpathians (CWC). In the CWC, Mesozoic alkaline volcanism is known from the Tatric (envelope) and Fatric Superunits (Krížna, Manín and Klape Units, Plašienka 1999). On the basis of stratigraphic data, the age of the volcanics under consideration is Barremian–Aptian, which is proved also by the K/Ar method applied to hornblende and clinopyroxene concentrate, and the whole rock (102 Ma, Spišiak & Balogh 2002). The K/Ar method applied to hornblende and clinopyroxene concentrate and the whole rock proved the Aptian–Albian age (116 ± 6.5 and 106.2 ± 1.7 Ma) of volcanic activity in the Krížna Nappe (Bujnovský et al. 1981). The products of the volcanic activity are low differentiated basalts/basanites, or very rarely picrites. Volcaniclastic rocks are present in substantial amounts (hyaloclastites, etc.). The majority of Mesozoic alkaline rocks (except for picrites) are characterized by the presence of a fine-grained devitrified matrix (up to 40 vol. %). Olivines are completely replaced by chlorite-serpentine-carbonate aggregates. Clinopyroxenes are dom-

inating minerals in all rock types. Besides phenocrysts of various shape and size, they also form microlites in the devitrified matrix. Kearsutite, albite, apatite, analcime, pseudoleucite, spinel, ore minerals, and Ti-biotite are rarely present (Spišiak & Hovorka 1997). Based on alkali character of volcanics, Cretaceous volcanism of CWC as well as EWC is associated with short-living rifting (Hovorka & Spišiak 1988). The studied rock types are represented mostly by hyaloclastites and autometamorphosed basalts.

In this contribution we studied Cr-spinels and clinopyroxene phenocrysts from the following localities in the CWC: Podmanín, Košeca, Dobrá, Slopná, Štepnica, Osobitá and Čebraď (Fig. 1). A majority of the studied localities are situated in the Strážovské vrchy Mts (Podmanín, Slopná, Dobrá and Košeca). The Štepnica locality is situated in the Javorníky Mts, Čebraď belongs to the Chočské vrchy Mts, and Osobitá is located in the Tatry Mts. Hyaloclastite bodies in Podmanín and Slopná belong to the Manín Tectonic Unit. The surrounding rocks are Lower Albian cherty limestones of the Jelenia skala Formation and thin-rhythmic flysch sediments of the Praznov Formation (Cenomanian–Middle Turonian). The stratigraphic age of the hyaloclastite body is Early Albian (Mello et al. 2005). The basalt body near Dobrá is situated between organodetrital limestones with interbeds of cherts (Baremian–Lower Aptian) and patchy marls with foraminifers of Late Albian–Early Cenomanian age. This sedimentary sequence with the volcanic body belongs to the Fatric Superunit (Krížna Nappe). The stratigraphic age of the volcanic rock is probably Early Albian. Another Fatric basalt hyaloclastite body is situated near Košeca. The surrounding rocks are marly limestone of Late Jurrasic–Early Cretaceous age. The hyaloclastite contains clasts of Hauterivian and Barremian limestones. The assumed age of the volcanism is probably Albian. Volcanics in Čebraď (Krížna Nappe) are represented by basaltic breccias and massive autometamorphosed basalts. The sedimentary sequence and the age of the volcanic rock are similar to those of the Košeca locality. The hyaloclastite body in Štepnica is embedded in marls of the Púchov Formation (Lower Albian–Lower Campanian). This formation is part of the Pieniny Klippen Belt and belongs to the Czorsztyn Tectonic Unit, Púchov — Jarmuta Group (Mello et al. 2005). Several hyaloclastite bodies in Osobitá are situated in Tithonian Sobótka Limestones (Lefeld 1985). Superincumbent beds of volcanites are found in the Osobitá chert limestones (Valanginian–Aptian). This rock sequence belongs to the Tatric Tectonic Unit.

Petrographic description

The size of spinel grains (octahedral crystals and fragments) is in average about 0.3–0.5 mm. Spinel phenocrysts are of black colour. They are clearly homogeneous in the reflected light. Cr-spinels of volcanic origin (see

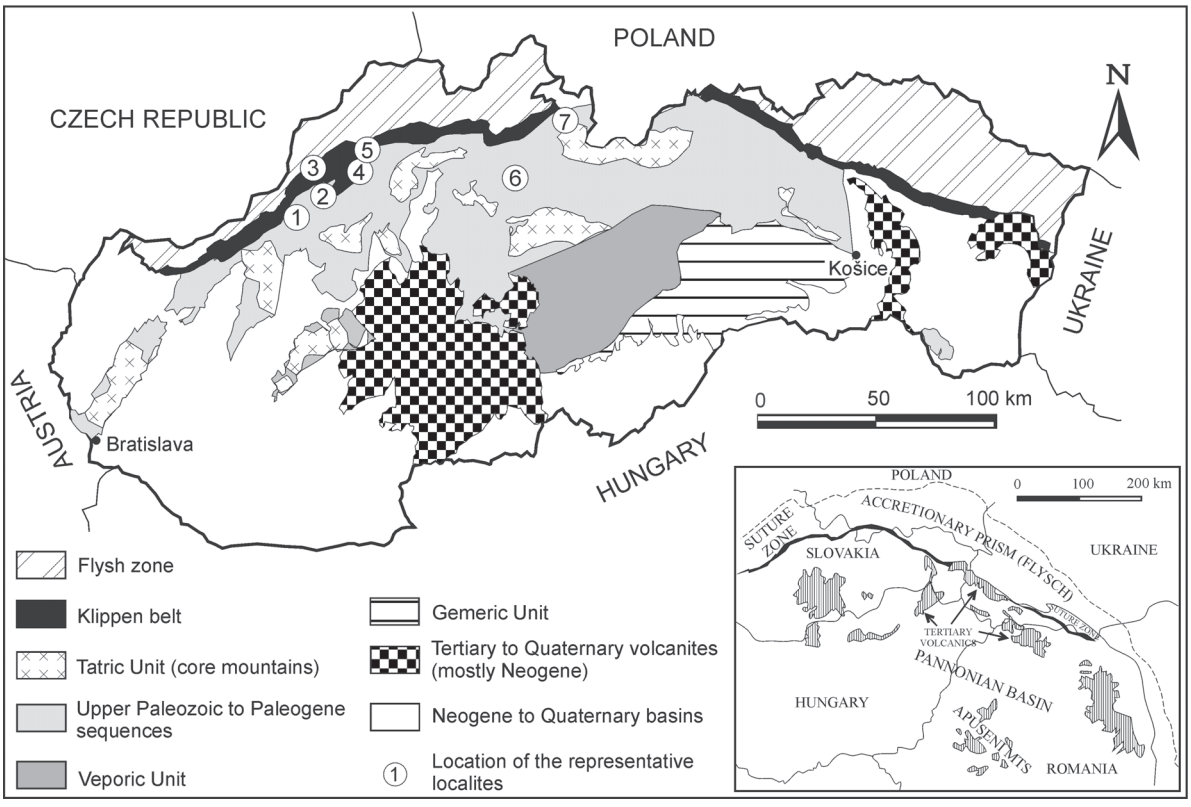

Fig. 1. Geological position of the studied localities in the simplified geological map of the Western Carpathians. Localities studied: **1** — Dobrá, **2** — Košeca, **3** — Štepnica, **4** — Slopná, **5** — Podmanín, **6** — Čebraď, **7** — Osobitá.

spinel composition) from Podmanín and Čebraď have very similar characteristic features: a — oscillatory zoning (Fig. 2a); b — silicate/melt inclusions (Fig. 2b,c).

Silicate and melt inclusions trapped in spinel were found only in volcanic Cr-spinel from Podmanín and Čebraď. The shape of the inclusions is dominantly convex oval and their size is up to 40 µm. The inclusions with cracks are altered and filled with secondary chlorite and calcite (Fig. 2b). Most of the inclusions contain two phases: daughter clinopyroxene (cpx) + plagioclase (Fig. 2b) or daughter cpx crystal + glass + shrinkage vapour bubble (Fig. 2c). Single-phase inclusions contain cpx or glass. Clinopyroxene inclusions in Cr-spinel host were observed as single individual euhedral crystals, usually occurring along the inclusions contact with the host spinel. Generally, daughter cpx inclusions are surrounded by residual glass containing circular cells which are most probably a result of vapour exsolution from the entrapped melt (Fig. 2c).

Fe-Ti spinels are associated with clinopyroxene (cpx) phenocrysts and apatite in the Dobrá and Štepnica localities (Fig. 2d,e,f).

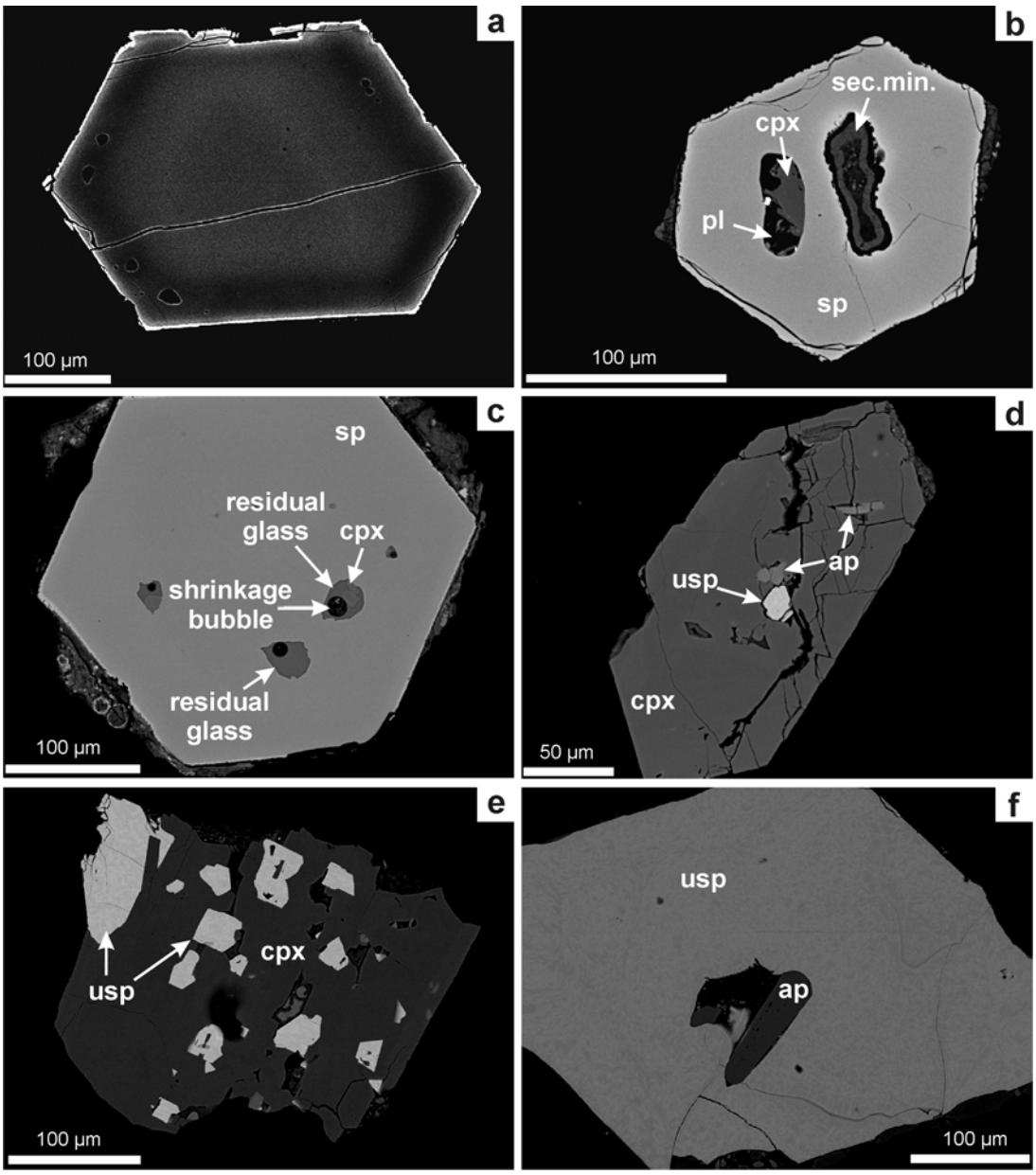

Fig. 2. a — Primary magmatic zoning of Cr-spinel of volcanic origin with melt inclusions from Podmanín; **b** — Inclusion of plagioclase (pl) with clinopyroxene (cpx) in Cr-spinel (sp) of volcanic origin and inclusion filled by secondary minerals (Čebraď locality); **c** — Inclusions of basaltic melt with clinopyroxene (cpx) and shrinkage bubbles in volcanic spinel (Podmanín); **d** — Euhedral clinopyroxene phenocryst with inclusion of apatite (ap) and Fe-Ti spinel (ulvöspinel-usp) from Dobrá locality; **e** — Impregnations of Fe-Ti spinel (usp) in clinopyroxene (cpx) grain from Štepnica; **f** — Inclusions of apatite (ap) in Fe-Ti spinel (usp) from Štepnica. BSE images.

Altered spinels were recognized among spinels of volcanic origin. The textures of altered spinels are heterogeneous (Fig. 3b,c,d) and porous (Fig. 3b,d). Enriched rims were observed very often (enrichment in TiO_2, Fe_2O_3 or Cr_2O_3, Fig. 3a). The strongest changes in spinel chemistry due to the alteration process were observed in Košeca, where almost all the spinel grains are altered. Alteration affects spinel grains from their margins and alteration progresses faster in spinel grains containing microfractures.

Clinopyroxene phenocrysts were found in heavy mineral fractions from Štepnica, Dobrá and Podmanín. The euhedral phenocrysts are up to 1.5 mm in size and are brown (Štepnica, Dobrá) or green (Podmanín) in colour. Oscillatory zonation is quite usual in cpx phenocrysts from Štepnica and Dobrá (Fig. 4). Several oscillatory zoned cpx grains consist of an anhedral homogeneous core with different chemical composition (Fe-rich cores). The boundary between core and zoned mantle is sharp (Fig. 4a,b) and the cores are magmatically corroded.

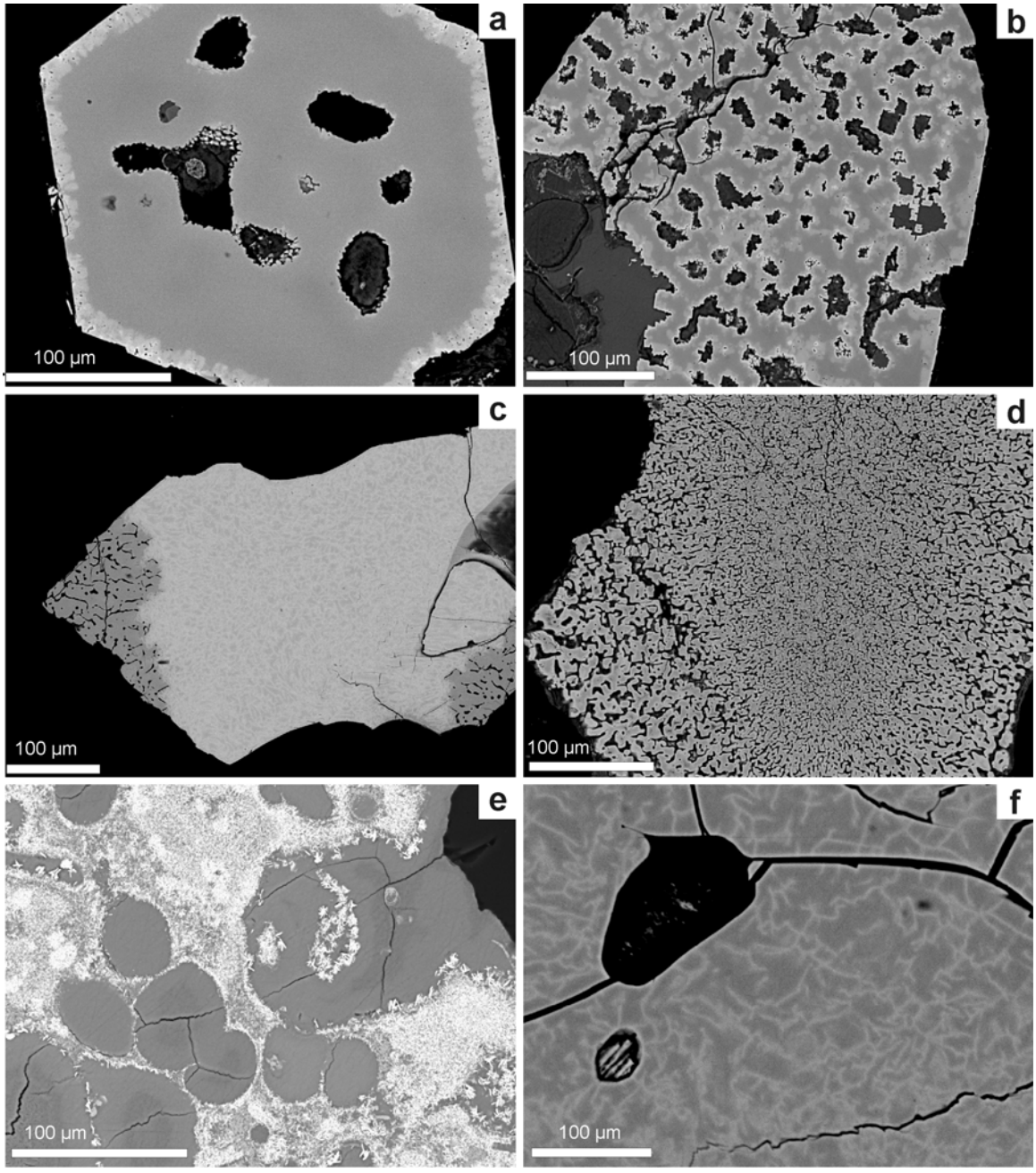

Fig. 3. Textures of altered spinels from Podmanín (a), Košeca (b,e), Slopná (c), Dobrá (d), Štepnica (f). BSE images. **a** — Euhedral Cr-spinel grain with altered rim. **b** — Heterogeneous Cr-spinel with porous structure. Pores are filled with secondary minerals. Altered phase is located around the pores. **c** and **d** — Decomposition of heterogeneous Cr-spinel structure. **e** — Almost completely altered Cr-spinel grain. White phase corresponds to Cr-magnetite. **f** — Heterogeneous Fe-Ti spinel. Lighter phase is enriched in TiO_2.

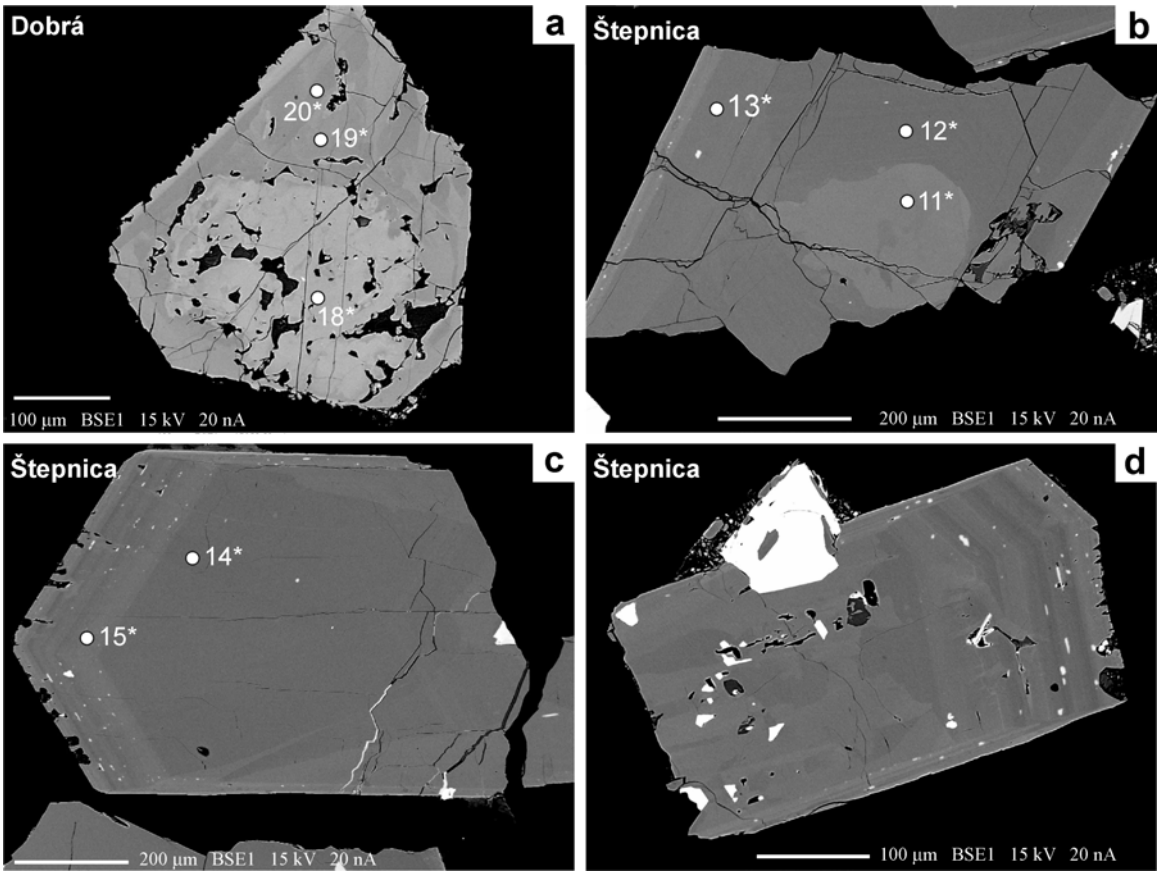

Fig. 4. Oscillatory zonation of cpx phenocrysts. Several cpx grains contain Fe-rich core with chemical composition different from that of younger zoned cpx (a,b). Numbers correspond to analyses in Table 4.

Analytical methods

Spinel and clinopyroxene were hand-picked from 10–15 kg of crushed volcanic rock (fraction <2 mm). Individual crystals were mounted in epoxy resin, polished and coated with carbon.

Spinel, silicate melt inclusions and clinopyroxene were analysed with a wave-dispersion (WDS) electron microprobe and photographed in back-scattered electrons (BSE) at the Department of Mineralogy in the Natural History Museum, London (UK). The microprobe used was a Cameca SX50 probe. The operating conditions were as follows: 20 kV accelerating voltage, 20 nA beam current, beam diameter 2–5 µm, ZAF corrections, standards (*n — natural, sy — synthetic*) — TiO_2 (*sy*) and $CaTiO_3$ (*sy*) for Ti, V (*sy*) for V, wollastonite (*n*) for Ca, Cr_2O_3 (*sy*) for Cr, Mn (*sy*) for Mn, hematite (*sy*) for Fe, Co (*sy*) for Co, Ni (*sy*) for Ni, sphalerite (*sy*) for Zn, corundum (*sy*) for Al, diopside (*n*) for Si, MgO_2 (*sy*) for Mg, jadeite (*n*) for Na, KBr (*sy*) for K, halite (*sy*) for Cl. A defocused beam could not be used for the melt inclusions analyses due to their small size. The Cpx phenocrysts were analysed with a Cameca SX100 probe at the Geological Survey of the Slovak Republic (Bratislava) under the following conditions: 15 kV accelerating voltage, 20 nA beam current, beam diameter 2–5 µm, ZAF corrections, standards (*n — natural, sy — synthetic*) — albite (*n*) for Na, wollastonite (*n*) for Si and Ca, Al_2O_3 (*sy*) for Al, orthoclase (*n*) for K, rodonite (*n*) for Mn, hematite (*n*) for Fe, MgO (*sy*) for Mg, TiO_2 (*sy*) for Ti, nickel (*sy*) for Ni, chromite (*n*) for Cr.

Fe^{2+} and Fe^{3+} in spinels were calculated assuming an ideal stoichiometry. Fe^{3+} in clinopyroxenes was calculated according to charge balance proposed by Ryburn et al. (1976) and Papike (1974).

Thermometric calculation with a combination of two thermometers was used for clinopyroxene inclusion in Cr-spinel. A QUILF software written by Andersen et al. (1995) was used for cpx–sp pairs. The results from QUILF equilibrium are compared with a single clinopyroxene thermometer proposed by Mercier (1976). For pyroxene barometry a barometer proposed by Nimis (1995) was used.

Microprobe analyses of residual glass were normalized to 100 %. Modal proportions of cpx and residual glass were calculated in the first step using BSE images. It is not possible to estimate the volume of spinel crystallized from the entrapped melt. Therefore 1, 3, 6 and 9 % of spinel component was added to homogenized components (glass+cpx). Final melt composition was plotted on a model curve in the TAS (total alkali vs. silica) diagram. The estimated primary melt composition is influenced by the following factors:

- Volumetric phase ratios do not respect the third dimension.

• The contents of alkalis are underestimated due to a focused electron beam used in the WDS analyses.

Results

Spinel composition

The spinels from Mesozoic alkali volcanics show a significant variation in chemistry, mainly in terms of the most important parameters such as Mg# ($Mg/Mg+Fe^{2+}$), Cr# ($Cr/Cr+Al$), TiO_2 and Fe^{2+}/Fe^{3+} (Table 1). These variations suggest multiple sources of the spinels. To distinguish between spinels from these sources (hereafter, peridotitic and volcanic), the most useful variables are TiO_2 content with a combination of the Fe^{2+}/Fe^{3+} ratio in spinels (Lenaz et al. 2000; Kamenetsky et al. 2001). "Mantle" spinels (from ophiolitic peridotites and mantle xenoliths) have statistically (>95 %) lower TiO_2 (<0.2 wt. %) and higher Fe^{2+}/Fe^{3+} (>3) over the whole interval in Al_2O_3 (6–56 wt. %) than volcanic spinels (Kamenetsky et al. 2001). Volcanic spinels with TiO_2 <0.2 wt. % are uncommon (some suites of low-Ti MORB, arc tholeiites and boninites) and those with TiO_2 <0.1 are exceptionally rare (some low-Ca boninites). Lenaz et al. (2000) have set a compositional boundary between the peridotitic and volcanic spinels at TiO_2 = 0.2 wt. %. Volcanic spinels tend to have the Fe^{2+}/Fe^{3+} ratio usually up to four (Kamenetsky et al. 2001).

Several principal compositional groups have been distinguished according to chemical composition (Fig. 5): **1.** mantle peridotitic spinel (Podmanín, Dobrá and Slopná localities); **2.** volcanic spinel: a — Cr-spinel (Podmanín, Dobrá, Slopná, Košeca and Čebraď localities); b — Fe-Ti spinel (Podmanín, Dobrá, Štepnica and Osobitá localities); **3.** altered spinel (all localities studied).

Peridotitic spinel is characteristic of the highest Al_2O_3 content (up to 60 wt. %, e.g. Podmanín). TiO_2 content is usually very low (<0.10 wt. %). Mg# ($Mg/Mg+Fe^{2+}$) values are 79–81 mol % and Cr# ($Cr/Cr+Al$) ranges between 7 and 12 mol %. Peridotitic spinels from Dobrá show the lowest content of Al_2O_3 (36–48 wt. %) in this compositional group (Table 1, Fig. 6). An interesting spinel phase, with up to 50 wt. % Cr_2O_3, was recognized as tiny inclusions (up to 10 μm) within Cr-diopside phenocrysts from Podmanín.

Among volcanic spinels, those from Podmanín and Čebraď show very similar chemical compositions. Al_2O_3 content ranges from 24 to 39 wt. % and TiO_2 content is between 0.9 and 1.1 wt. %. Mg# values range between 71 and 74 mol % and Cr# values correspond to 28–35 mol % (Table 1). Oscillatory zoning of volcanic Cr-spinels from Podmanín and Čebraď is caused by different content of trivalent cations (Al^{3+}, Cr^{3+}) in individual zones. Autometamorphosed basalt from Čebraď contains only volcanic Cr-spinel, which contains the highest TiO_2 content (up to 1.84 wt. %).

Fe-Ti spinels (titanomagnetites) have been found in Podmanín, Dobra, Štepnica and Osobitá (Table 2). The major constituent is magnetite. The amount of the ulvöspinel (usp) component is between 8 and 38 mol %. Almost all studied samples of Fe-Ti spinels show Al_2O_3 content about 3 wt. % in average. A complete chromian spinel–titanomagnetite (Fe-Ti spinel) solid solution has not been observed.

Detrital Cr-spinels of volcanic origin from the Poruba flysch Fm in general are different in terms of Al_2O_3 content, Mg# and Cr# to those of alkali basalts. Detrital Cr-spinels have lower Al_2O_3 content (6.11–30.58 wt. %) and most

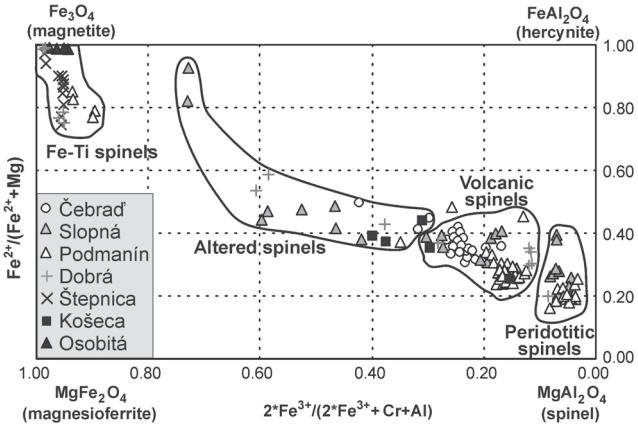

Fig. 5. Nomenclature and composition of spinels from Mesozoic alkali volcanic rocks based on the classification of Deer et al. (1992).

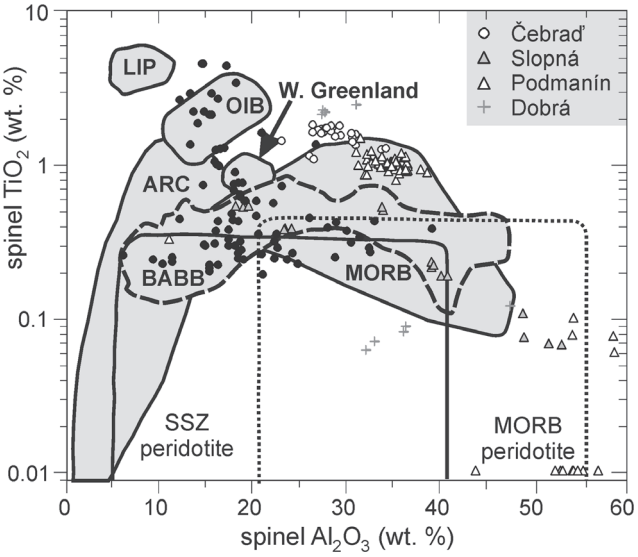

Fig. 6. Al_2O_3 vs. TiO_2 compositional relationships in spinel from the Mesozoic alkali volcanic rocks. Compositional fields of spinels from volcanic environments (MORB — mid-ocean ridge basalt, OIB — ocean-island basalt, LIP — large igneous provinces, ARC — island arc magmas, BABB — back-arc basin basalt) are compared with spinels from mantle (SSZ and MORB — dot line) peridotites (according to Kamenetsky et al. 2001). BABB field is restricted by a dashed line from Lenaz et al. (2000). Analyses of detrital spinels of volcanic origin (black circles) from mid-Upper Cretaceous flysch sedimets in the Western Carpathians are plotted for comparison.

Table 1: Representative microprobe analyses of Cr-spinels from Mesozoic alkali volcanics.

Type	**Volcanic spinel**													**Peridotitic spinel**						
locality	**Čebraď**				**Podmanín**			**Dobrá**			**Slopná**			**Podmanín**			**Dobrá**		**Slopná**	
zone	**rim**	**core**	**core**	**rim**	**rim**	**core**	**rim**	**core**	**rim**	**–**		**–**	**–**	**–**	**–**	**–**	**–**	**–**	**–**	**–**
analysis	**1**	**2**	**4**	**5**	**88**	**71**	**72**	**4**	**5**	**7**	**102**	**1**	**7**	**1**	**4**	**7**	**40**	**6**	**109**	**5**
SiO_2	0.09	0.08	0.15	0.08	0.20	0.17	0.18	0.11	0.16	0.14	0.10	0.01	0.03	0.05	0.04	–	0.04	0.04	0.00	0.00
TiO_2	1.74	1.60	1.27	1.82	0.94	1.10	1.06	2.30	2.49	2.17	1.01	0.51	0.39	0.34	0.08	0.01	0.09	0.12	0.19	0.07
Al_2O_3	27.92	31.71	34.42	29.85	38.69	32.87	36.58	27.98	31.69	27.89	35.00	34.60	24.60	11.01	59.75	54.21	37.07	48.42	40.97	52.65
Cr_2O_3	29.40	26.84	24.22	26.58	24.12	29.88	25.73	26.99	21.88	28.02	28.37	31.61	37.30	50.45	7.16	13.29	27.79	18.27	25.30	14.57
Fe_2O_3*	12.43	11.66	10.79	12.82	7.93	7.78	8.05	14.01	14.54	13.08	6.89	3.31	9.34	11.76	1.76	2.50	5.87	4.49	3.60	2.24
FeO	14.10	13.82	12.98	13.51	11.23	11.92	11.38	15.25	14.73	14.53	11.81	15.49	12.03	16.83	8.54	10.00	12.48	8.69	11.40	11.07
MnO	0.21	0.20	0.19	0.24	0.14	0.19	0.19	0.25	0.25	0.25	0.18	0.36	0.24	0.79	0.12	0.06	0.16	0.20	0.15	0.13
MgO	14.40	15.08	15.70	14.77	17.58	16.38	17.08	13.68	14.25	14.03	16.64	14.01	15.17	10.50	21.13	19.94	16.38	20.12	17.27	18.88
CaO	0.01	0.02	0.01	0.04	0.00	0.00	0.02	0.00	0.01	0.02	0.00	0.00	0.01	0.28	0.00	0.00	0.00	0.01	0.03	0.00
ZnO	0.00	0.14	0.05	0.11	0.08	0.08	0.11	0.00	0.05	0.04	0.04	0.24	0.03	0.35	0.02	0.00	0.14	0.09	0.18	0.20
V_2O_5	0.20	0.23	0.13	0.17	0.18	0.21	0.21	–	–	–	0.17	–	–	0.00	–	–	0.18	–	0.20	–
total	100.50	101.35	99.92	100.00	101.10	100.57	100.58	100.56	100.06	100.15	100.22	100.15	99.15	102.36	98.60	100.00	100.20	100.46	99.29	99.80
formula based on 3 cations																				
Si	0.003	0.002	0.004	0.002	0.006	0.005	0.005	0.003	0.005	0.004	0.003	0.000	0.001	0.002	0.001	–	0.001	0.001	0.000	0.000
Ti	0.039	0.035	0.028	0.041	0.020	0.024	0.023	0.052	0.055	0.049	0.022	0.011	0.009	0.008	0.001	0.000	0.002	0.002	0.004	0.001
Al	0.982	1.087	1.176	1.044	1.273	1.118	1.222	0.989	1.105	0.987	1.182	1.188	0.881	0.418	1.817	1.675	1.244	1.521	1.356	1.648
Cr	0.694	0.617	0.555	0.624	0.533	0.682	0.576	0.640	0.512	0.665	0.643	0.728	0.896	1.286	0.146	0.276	0.625	0.385	0.562	0.306
Fe^{3+}	0.279	0.255	0.235	0.286	0.167	0.169	0.172	0.316	0.324	0.296	0.149	0.072	0.214	0.285	0.034	0.049	0.126	0.090	0.076	0.045
Fe^{2+}	0.352	0.336	0.315	0.335	0.262	0.288	0.270	0.382	0.364	0.365	0.283	0.377	0.306	0.454	0.184	0.219	0.297	0.194	0.268	0.246
Mn	0.005	0.005	0.005	0.006	0.003	0.005	0.005	0.006	0.006	0.006	0.004	0.009	0.006	0.022	0.003	0.001	0.004	0.005	0.004	0.003
Mg	0.641	0.654	0.678	0.654	0.732	0.705	0.722	0.611	0.628	0.628	0.711	0.609	0.687	0.505	0.813	0.779	0.695	0.800	0.723	0.747
Zn	0.000	0.003	0.001	0.002	0.002	0.002	0.002	0.000	0.001	0.001	0.001	0.005	0.001	0.008	0.000	0.000	0.003	0.002	0.004	0.004
V	0.004	0.004	0.002	0.003	0.003	0.004	0.004	–	–	–	0.003	–		–	–	–	0.003	–	0.004	–
Cr#	41	36	32	37	29	38	32	62	63	63	35	38	50	75	7	14	70	81	29	16
Mg#	65	66	68	66	74	71	73	39	32	40	72	62	69	53	82	78	33	20	73	75
Fe^{2+}/Fe^{3+}	1.26	1.32	1.34	1.17	1.57	1.70	1.57	1.21	1.13	1.23	1.90	5.21	1.43	1.59	5.38	4.44	2.36	2.15	3.52	5.50

*Fe_2O_3 calculated from stoichiometry.

of them have higher Cr# (60–87 mol %) and lower Mg# (34–63 mol %) (Table 3).

Inclusions within Cr-spinel

Clinopyroxene inclusions

Cpx inclusions within Cr-spinel from Podmanín and Čebraď correspond to augite and diopside according to the classification by Morimoto (1989). In comparison to cpx phenocryst from Štepnica, Dobrá and Podmanín, the cpx inclusions have higher TiO_2 (3.08–4.26 wt. %) and Al_2O_3 (7.50–11.61 wt. %) contents. The Na_2O content is of about 0.70 wt. % in average (Table 4). A higher content of Cr_2O_3 in some cpx inclusion analyses is caused by host-spinel contamination.

The QUILF program (Andersen et al. 1995) and a single cpx thermometer proposed by Mercier (1976) which refer to hypothetical spinel (as an associated crystallized phase) were used for thermometric calculations based on Mg-Fe partitioning between host spinels and cpx inclusions in Podmanín. The QUILF data show the temperature of cpx crystallization between 1143–1183 ºC corresponding to a pressure of 0.50–0.68 GPa (Nimis 1995). The minimum temperature ac-cording to Mercier's thermometer corresponds to 1023–1175 ºC.

Plagioclase and melt inclusions

Plagioclase was found only as inclusions in Cr-spinel. Albite end-member is dominant (81.40 mol %) in the plagioclase inclusion from Čebraď. This albite is probably not primary magmatic material, but it could be a product of secondary hydrothermal alteration of the basalt body.

Most of the residual glass analyses project on the border of trachybasalt–basalt field in the TAS diagram (Fig. 7). One analysis corresponds to basanite–tephrite. All the residual glass analyses are situated above the boundary defining alkali basalt (Irvine & Baragar 1971). The bulk melt compositions show a drift to lower Na_2O+K_2O values into the basalt field. Addition of x % (x = 1–9%) spinel into the phase assemblage of the silicate melt and cpx inclusions will cause a decrease in SiO_2 content and drift to picrobasalt or basanite fields. The composition of parental magma could be derived from bulk melt composition. The residual glass and bulk melt compositions suggest alkali character of the magma. The bulk melt composition shows the

Table 2: Representative microprobe analyses of Fe-Ti spinels from Mesozoic alkali volcanics.

Locality	Štepnica						Osobitá			Podmanín			Dobrá		
analysis	80	81	82	86	88	89	90	95	69	70	71	72	89	90	93	94	30	32	33	34
SiO_2	0.18	0.13	0.16	0.12	0.00	0.00	0.00	0.00	0.38	0.23	0.21	0.18	0.21	0.18	0.28	0.47	0.05	0.10	0.11	0.06
TiO_2	14.14	14.57	14.17	14.59	7.46	8.12	7.52	14.06	14.32	15.13	14.87	14.52	14.06	14.03	16.67	16.93	3.18	14.31	7.82	7.84
Al_2O_3	2.98	3.15	2.90	3.10	0.80	1.22	0.98	3.11	1.84	3.64	3.64	2.75	4.25	4.24	6.41	6.42	1.05	2.90	0.75	0.76
Cr_2O_3	0.03	0.07	0.06	0.00	0.04	0.02	0.02	0.07	0.01	0.03	0.02	0.01	0.14	0.11	0.06	0.03	0.03	0.05	0.03	0.00
Fe_2O_3*	50.51	52.20	50.79	51.78	60.53	59.08	59.17	50.98	51.45	48.64	49.43	50.70	50.24	50.79	45.48	45.77	64.14	51.92	60.06	59.68
FeO	27.06	23.45	26.73	23.12	27.39	28.02	28.36	25.86	29.04	28.97	29.18	29.34	26.37	26.42	24.76	25.15	28.95	23.96	29.51	29.25
MnO	1.56	0.88	1.66	0.74	1.13	1.16	1.36	1.68	0.19	0.18	0.13	0.16	0.57	0.61	0.41	0.57	1.90	0.90	1.21	1.32
MgO	1.39	4.43	1.59	4.41	1.32	0.95	0.46	2.04	0.02	0.08	0.01	0.02	2.82	2.88	4.15	3.98	0.00	3.85	0.11	0.12
CaO	0.04	0.02	0.04	0.24	0.02	0.02	0.00	0.06	0.01	0.01	0.04	0.03	0.05	0.05	0.06	0.01	0.02	0.07	0.00	0.00
ZnO	0.16	0.11	0.11	0.09	0.29	0.22	0.17	0.24	0.06	0.12	0.09	0.01	0.09	0.09	0.03	0.21	0.19	0.13	0.24	0.16
V_2O_5	–	–	–	–	0.13	0.18	0.10	0.36	0.88	0.98	1.07	0.86	0.23	0.28	0.39	0.36	0.09	0.24	0.20	0.11
CoO	–	–	–	–	–	–	–	–	0.04	0.06	0.07	0.08	–	–	–	–	–	–	–	–
total	98.06	98.99	98.20	98.18	99.11	98.99	98.13	98.46	98.24	98.07	98.76	98.68	99.01	99.66	98.70	99.91	99.60	98.42	100.03	99.30
formula based on 3 cations																				
Si	0.007	0.005	0.006	0.004	0.000	0.000	0.000	0.000	0.015	0.009	0.008	0.007	0.008	0.006	0.010	0.017	0.002	0.004	0.004	0.002
Ti	0.406	0.405	0.406	0.409	0.215	0.234	0.220	0.401	0.419	0.439	0.429	0.421	0.393	0.390	0.458	0.460	0.092	0.403	0.225	0.228
Al	0.134	0.137	0.130	0.136	0.036	0.055	0.045	0.139	0.084	0.165	0.164	0.125	0.186	0.184	0.276	0.273	0.048	0.128	0.034	0.034
Cr	0.001	0.002	0.002	0.000	0.001	0.001	0.001	0.002	0.000	0.001	0.000	0.001	0.004	0.003	0.002	0.001	0.001	0.001	0.001	0.000
Fe^{3+}	1.451	1.451	1.456	1.451	1.745	1.707	1.733	1.453	1.504	1.411	1.425	1.469	1.405	1.411	1.249	1.243	1.856	1.461	1.732	1.734
Fe^{2+}	0.864	0.725	0.852	0.720	0.878	0.900	0.923	0.819	0.944	0.934	0.934	0.945	0.820	0.816	0.755	0.759	0.931	0.749	0.946	0.944
Mn	0.050	0.028	0.054	0.023	0.037	0.038	0.045	0.054	0.006	0.006	0.004	0.005	0.018	0.019	0.013	0.017	0.062	0.028	0.039	0.043
Mg	0.079	0.244	0.090	0.245	0.075	0.054	0.027	0.115	0.001	0.005	0.001	0.001	0.156	0.158	0.226	0.214	0.000	0.214	0.007	0.007
Zn	0.005	0.003	0.003	0.002	0.008	0.006	0.005	0.007	0.002	0.003	0.003	0.000	0.002	0.002	0.001	0.006	0.005	0.004	0.007	0.004
V	–	–	–	–	–	0.003	0.003	0.009	0.023	0.025	0.027	0.022	0.006	0.007	0.009	0.009	0.002	0.006	0.005	0.003

*Fe_2O_3 calculated from stoichiometry.

$Al_2O_3/(CaO+Na_2O+K_2O)$ ratio in the range of 0.70–0.97 and the $Al_2O_3/(Na_2O+K_2O)$ ratio in the range of 3.45–4.75, thus corresponding to metaluminous melt. Selected electron-microprobe analyses of the residual melt are listed in Table 5.

Clinopyroxene phenocrysts

Cpx phenocrysts from Štepnica and Dobrá correspond to diopside according to the classification by Morimoto (1989). Their composition is slightly different from that of cpx inclusions in Cr-spinel. Cpx phenocrysts have a lower content of TiO_2 (up to 2.16 wt. %) and a lower Al_2O_3 content (2.2–5.94 wt. %). Their zonation is a consequence of small differences in Al_2O_3 (e.g. 2.31–3.65 wt. %), TiO_2 (e.g. 1.16–1.73 wt. %), FeO and MgO contents in individual zones. The Al^{VI}/Al^{IV} ratio is always less than 1. Calculated pressures according the pyroxene barometer by Nimis (1995) correspond to 0.41–0.69 GPa.

The distinct compositional differences in terms of TiO_2, FeO, MnO, MgO and Na_2O contents have been observed between homogeneous cores and zoned rims. Cores are enriched in FeO (10.44 wt. %), MnO (0.54 wt. %) and Na_2O (1.94 wt. %) in comparison with rims. The Al^{VI}/Al^{IV} ratio is always above 1. On the other hand, zoned cpx rims are enriched in TiO_2 (2.16 wt. %), and MgO compared to cores (Fig. 4, Table 4). Barometric calculation for one of these cores yielded the value of 1.15 GPa.

Cpx phenocrysts with exsolved lenticular cpx lamellas occur rarely in Dobrá. This cpx has the highest Al_2O_3 content (6.70 wt. %) and the lowest FeO content (2.56 wt. %). The exsolved cpx contains up to 4.88 wt. % Al_2O_3 and 1.99 wt. % of CaO. These cpx correspond to enstatite (En_{85-88} mol %, Fs_{11} mol %, Wo_{1-4} mol %).

The cpx phenocrysts from Podmanín have the lowest TiO_2 (up to 0.81 wt. %) and Al_2O_3 (0.62–1.44 wt. %) contents. On the other hand, they have remarkable contents of Cr_2O_3 (0.66–2.02 wt. %) and could be classified as Cr-diopside. Na_2O content is usually the highest (up to 2 wt. %). Cr-diopsides have the highest Al^{VI}/Al^{IV} ratio (1.56–3.30). Cr-diopside phenocrysts are rarely heterogeneous (small differences in SiO_2, Al_2O_3, TiO_2, FeO contents). The calculated pressures using the barometer of Nimis (1995) correspond to 1.34–1.48 GPa.

Table 3: Representative microprobe analyses of Cr-spinels of volcanic origin from the Poruba Flysch Formation.

Locality	Bystrička					Čutkov potok					Čavoj				Boboty			
analysis	38	45	51	56	62	78	24	3	5	14	1	4	6	18	23	37	38	41	47
SiO_2	0.00	0.02	0.02	0.05	0.02	0.07	0.02	0.04	0.02	0.01	0.02	0.10	0.07	0.03	0.02	0.01	0.04	0.02	0.03
TiO_2	2.27	0.27	0.39	0.72	0.67	0.25	0.62	0.81	0.25	0.79	0.30	0.33	0.33	2.38	0.24	0.34	0.31	1.04	0.46
Al_2O_3	15.36	6.11	16.04	18.04	18.74	23.71	19.29	18.88	18.43	12.13	18.04	22.71	30.58	18.74	13.62	24.94	17.47	14.85	16.46	12.12
Cr_2O_3	37.09	58.72	46.16	40.61	42.48	44.46	40.97	41.07	39.84	44.74	40.52	41.92	35.03	45.00	36.44	39.20	46.35	47.69	39.19	51.17
Fe_2O_3*	14.95	6.20	8.37	9.65	7.73	3.87	9.08	9.29	5.90	16.38	11.49	5.54	5.39	5.42	16.36	6.04	5.94	9.26	13.33	6.89
FeO	21.28	18.55	18.78	22.83	21.25	12.99	17.80	17.63	19.99	19.12	18.08	17.70	11.86	18.85	22.85	14.32	20.07	16.02	20.92	19.65
MnO	0.39	1.00	0.24	0.40	0.34	0.23	0.27	0.24	0.24	0.30	0.30	0.32	0.18	0.32	0.43	0.23	0.32	0.25	0.33	0.39
MgO	7.98	8.34	9.46	6.64	7.89	14.30	10.74	10.84	9.29	8.14	9.82	10.86	16.06	10.00	6.62	13.58	9.21	11.69	8.52	8.87
ZnO	0.21	0.62	0.18	0.19	0.14	0.14	0.11	0.11	0.12	0.15	0.19	0.28	0.07	0.12	0.18	0.16	0.22	0.22	0.16	0.21
V_2O_5	0.83	0.29	0.43	0.58	0.54	0.28	0.39	0.40	0.30	0.87	0.62	0.38	0.18	0.36	0.76	0.27	0.34	0.29	0.54	0.33
total	100.37	100.11	100.37	99.71	99.80	100.30	99.28	99.31	99.27	99.80	99.86	100.04	99.79	99.19	99.65	98.99	100.26	100.61	100.51	100.12
formula based on 3 cations																				
Si	0.000	0.001	0.001	0.002	0.001	0.002	0.000	0.001	0.001	0.000	0.001	0.003	0.002	0.001	0.001	0.000	0.001	0.001	0.001	0.001
Ti	0.056	0.007	0.010	0.018	0.016	0.006	0.015	0.020	0.006	0.072	0.019	0.007	0.007	0.008	0.060	0.005	0.008	0.008	0.025	0.011
Al	0.596	0.246	0.613	0.699	0.716	0.846	0.726	0.712	0.702	0.479	0.684	0.835	1.057	0.710	0.541	0.901	0.663	0.559	0.631	0.473
Cr	0.965	1.583	1.183	1.055	1.089	1.064	1.035	1.038	1.143	1.055	1.031	1.035	0.812	1.144	0.971	0.950	1.180	1.205	1.008	1.339
Fe^{3+}	0.370	0.159	0.204	0.239	0.189	0.088	0.218	0.224	0.144	0.413	0.278	0.130	0.119	0.131	0.415	0.139	0.144	0.223	0.327	0.171
Fe^{2+}	0.586	0.529	0.509	0.628	0.576	0.329	0.475	0.471	0.540	0.536	0.487	0.462	0.291	0.507	0.644	0.367	0.541	0.428	0.569	0.544
Mn	0.011	0.029	0.007	0.011	0.009	0.006	0.007	0.007	0.007	0.009	0.008	0.008	0.005	0.009	0.012	0.006	0.009	0.007	0.009	0.011
Mg	0.392	0.424	0.457	0.325	0.382	0.645	0.511	0.517	0.447	0.406	0.471	0.505	0.702	0.479	0.333	0.621	0.442	0.557	0.413	0.438
Zn	0.005	0.016	0.004	0.005	0.003	0.003	0.002	0.003	0.003	0.004	0.005	0.006	0.001	0.003	0.004	0.004	0.005	0.005	0.004	0.005
V	0.018	0.006	0.009	0.013	0.012	0.006	0.008	0.008	0.006	0.019	0.013	0.008	0.004	0.008	0.017	0.005	0.007	0.006	0.012	0.007
Cr#	62	87	66	60	60	56	59	59	62	69	60	55	43	62	64	51	64	68	62	74
Mg#	40	44	47	34	40	66	52	52	45	43	49	52	71	49	34	63	45	57	42	45
Fe^{2+}/Fe^{3+}	1.6	3.3	2.5	2.6	3.1	3.7	2.2	2.1	3.8	1.3	1.7	3.5	2.4	3.9	1.6	2.6	3.8	1.9	1.7	3.2

*Fe_2O_3 calculated from stoichiometry.

Table 4: Representative microprobe analyses of clinopyroxenes from Mesozoic alkali volcanics.

Locality	**Čebraď**			**Štepnica**					**Dobrá**						**Podmanín**					
type	**inclusions in Cr-spinels**			**zoned phenocrysts**					**zoned phenocrysts**			**cpx**	**exsolved opx**		**inclusions in Cr-spinels**			**Cr-diopside phenocrysts**		
analysis	**1**	**4**	**9**	**11**	**12**	**13**	**14**	**15**	**18**	**19**	**20**	**5**	**1**	**4**	**37**	**38**	**48**	**1**	**2**	**3**
SiO_2	44.92	46.06	42.32	52.80	52.43	50.88	52.19	50.17	52.68	48.69	50.80	50.59	53.41	55.37	43.68	43.75	44.34	54.54	53.21	51.13
TiO_2	3.08	2.96	3.24	0.39	1.06	1.50	1.16	1.73	0.56	2.16	1.78	1.17	0.16	0.23	3.30	3.33	3.23	0.05	0.23	0.63
Al_2O_3	10.78	7.50	10.88	2.81	2.46	3.71	2.31	3.65	1.52	5.94	4.33	6.70	4.88	4.54	8.81	9.02	9.68	0.62	2.90	4.31
Cr_2O_3	1.08	0.76	0.91	0.07	0.02	0.00	0.02	0.02	0.15	0.51	0.39	0.81	0.49	0.50	0.68	0.65	0.72	2.02	0.98	0.89
FeO	8.73	5.32	6.69	10.44	7.85	7.88	6.92	7.72	10.28	6.16	6.13	2.56	7.06	7.01	6.07	5.99	6.30	3.28	4.87	6.23
MnO	0.19	0.12	0.09	0.54	0.20	0.20	0.24	0.19	0.36	0.09	0.16	0.10	0.19	0.19	0.11	0.08	0.09	0.25	0.19	0.23
MgO	13.02	14.04	11.94	11.77	14.03	13.31	14.44	13.58	12.91	14.20	14.96	14.24	31.47	31.15	14.04	13.86	14.24	16.10	15.73	14.46
CaO	16.02	21.58	21.41	20.94	23.00	23.01	23.56	23.04	22.43	22.52	22.95	21.77	0.52	1.99	20.69	20.79	20.28	21.67	19.91	19.87
Na_2O	1.78	0.83	0.86	1.94	0.86	0.96	0.71	0.91	0.99	0.59	0.50	1.49	0.05	0.11	0.70	0.75	0.77	1.69	1.57	1.35
K_2O	0.65	0.04	0.15	0.01	0.01	0.02	0.01	0.01	0.01	0.01	0.02	0.00	0.01	0.01	0.00	0.02	0.02	0.01	0.00	0.01
total	100.79	99.65	99.25	101.70	101.91	101.46	101.54	101.01	101.88	100.88	102.01	99.41	98.24	101.08	98.48	98.73	100.10	100.25	99.60	99.10
molar fraction of cations based on 6 oxygens																				
Si	1.6741	1.7205	1.6070	1.9514	1.9188	1.8756	1.9129	1.8595	1.9482	1.7939	1.8465	1.8511	1.8858	1.9043	1.6618	1.6580	1.6577	1.9901	1.9510	1.8995
Al^{IV}	0.1353	0.1303	0.1450	0.0486	0.0812	0.1244	0.0871	0.1405	0.0518	0.2061	0.1535	0.1489	0.1142	0.0957	0.1480	0.1487	0.1423	0.0022	0.0490	0.1005
Ti	0.3023	0.2108	0.3109	0.0109	0.0292	0.0415	0.0320	0.0484	0.0155	0.0599	0.0486	0.0321	0.0042	0.0058	0.2522	0.2572	0.2723	0.0170	0.0064	0.0176
Al^{VI}	0.0000	0.0000	0.0000	0.0737	0.0247	0.0366	0.0126	0.0188	0.0145	0.0519	0.0321	0.1400	0.0887	0.0883	0.0000	0.0000	0.0000	0.0000	0.0764	0.0880
Cr	0.0318	0.0224	0.0273	0.0020	0.0007	0.0000	0.0005	0.0006	0.0044	0.0150	0.0111	0.0235	0.0137	0.0135	0.0205	0.0195	0.0213	0.0581	0.0284	0.0262
Fe^{3+}	0.0400	0.0470	0.0637	0.0893	0.0581	0.0735	0.0606	0.0890	0.0725	0.0621	0.0489	0.0265	0.0070	0.0000	0.0555	0.0580	0.0334	0.0449	0.0431	0.0479
Fe^{2+}	0.2321	0.1192	0.1487	0.2335	0.1820	0.1694	0.1514	0.1502	0.2454	0.1278	0.1373	0.0518	0.2015	0.2016	0.1377	0.1318	0.1636	0.0553	0.1061	0.1458
Mn	0.0060	0.0038	0.0029	0.0169	0.0061	0.0061	0.0074	0.0059	0.0113	0.0027	0.0050	0.0029	0.0057	0.0054	0.0035	0.0026	0.0029	0.0077	0.0060	0.0071
Mg	0.7234	0.7818	0.6759	0.6486	0.7653	0.7315	0.7889	0.7504	0.7117	0.7798	0.8108	0.7767	1.6561	1.5973	0.7963	0.7830	0.7937	0.8756	0.8596	0.8007
Ca	0.6397	0.8637	0.8711	0.8292	0.9020	0.9086	0.9252	0.9149	0.8887	0.8891	0.8940	0.8536	0.0196	0.0734	0.8434	0.8442	0.8124	0.8474	0.7822	0.7911
Na	0.1286	0.0601	0.0633	0.1388	0.0607	0.0685	0.0505	0.0652	0.0707	0.0424	0.0352	0.1054	0.0037	0.0071	0.0516	0.0551	0.0558	0.1194	0.1118	0.0969
K	0.0309	0.0019	0.0073	0.0004	0.0005	0.0009	0.0007	0.0005	0.0004	0.0006	0.0008	0.0000	0.0003	0.0003	0.0000	0.0010	0.0010	0.0003	0.0000	0.0003
total	3.9444	3.9617	3.9231	4.0450	4.0291	4.0370	4.0304	4.0449	4.0364	4.0312	4.0245	4.0132	4.0035	3.9946	3.9706	3.9592	3.9564	4.0180	4.0215	4.0239
end members (mol %)																				
Johannsenite	0.35	0.21	0.16	0.91	0.32	0.32	0.39	0.32	0.59	0.15	0.27	0.16	–	–	0.19	0.14	0.16	0.41	0.32	0.39
Acmite	2.32	2.58	3.60	4.83	3.04	3.65	2.63	3.47	3.69	2.31	1.88	1.49	–	–	2.82	3.04	1.83	2.37	2.32	2.61
Jadeite	5.14	0.72	0.00	2.67	0.13	0.00	0.00	0.00	0.00	0.00	0.00	4.41	–	–	0.00	0.00	1.23	3.93	3.70	2.67
AlCaTs	0.00	0.00	0.00	2.63	1.16	1.95	0.66	1.00	0.76	2.82	1.71	3.42	–	–	0.00	0.00	0.00	0.00	2.64	2.13
FeCaTs	0.00	0.00	0.02	0.00	0.00	0.27	0.53	1.27	0.09	1.07	0.73	0.00	–	–	0.21	0.16	0.00	0.00	0.00	0.00
CrCaTs	1.85	1.23	1.55	0.11	0.04	0.00	0.03	0.03	0.23	0.81	0.59	1.31	–	–	1.12	1.07	1.17	3.06	1.52	1.43
TiCaTs	17.54	11.55	17.67	0.59	1.53	2.21	1.67	2.57	0.81	3.25	2.59	1.80	–	–	13.79	14.18	14.92	0.90	0.34	0.96
Wollastonite	17.38	34.34	30.11	40.58	44.18	43.63	45.02	43.46	43.89	40.24	41.74	41.06	1.04	3.91	30.80	30.98	28.26	40.29	37.23	38.22
Enstatite	41.96	42.84	38.42	35.06	40.07	38.95	41.17	39.90	37.13	42.40	43.19	43.45	87.62	85.07	43.54	43.16	43.48	46.14	46.22	43.65
Ferrosilite	13.46	6.53	8.46	12.62	9.53	9.02	7.90	7.99	12.81	6.95	7.32	2.90	11.34	11.02	7.53	7.27	8.96	2.91	5.71	7.95
Mg#	73	82	76	67	76	75	79	76	69	80	81	91	89	89	80	80	80	90	85	81

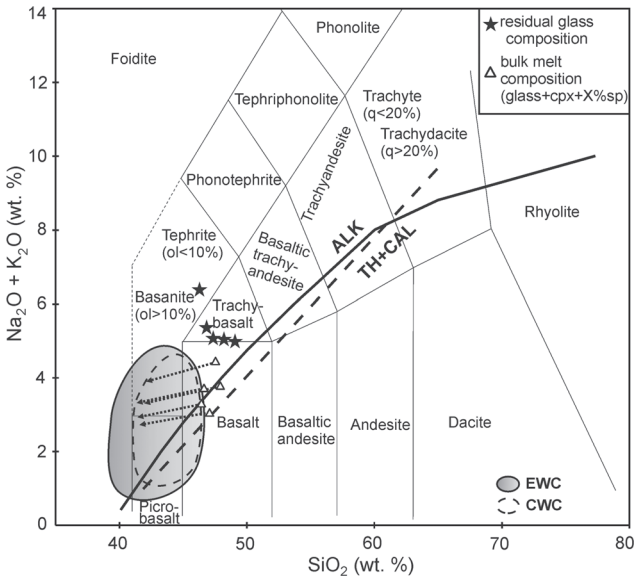

Fig. 7. Total alkali silica (TAS) diagram (Le Maitre et al. 1989) with projection points of melt inclusions in Cr-spinels from Podmanín. Dashed arrows indicate bulk melt composition with added different spinel content (1–9 %). Fields of Cretaceous basalts from the EWC and CWC are after Hovorka & Spišiak (1988), Hovorka et al. (1999), solid line–boundary between alkaline rocks (ALK) and tholeiites (TH) after Irvine & Baragar (1971), dashed line — after MacDonald & Katsura (1964). Other abbreviations: **q** — normative quartz; **ol** — normative olivine.

Table 5: Representative microprobe analyses of glass inclusions and albite in volcanic spinels.

Locality	Čebraď	Podmanín		
phase	alb	melt	melt	melt
analysis	12	39	41	43
SiO_2	63.92	46.98	44.67	45.75
TiO_2	0.05	2.71	2.98	2.61
Al_2O_3	26.21	16.61	16.22	16.25
Cr_2O_3	n.a.	0.58	0.56	0.70
MgO	0.03	3.33	9.04	6.97
MnO	n.a.	0.23	0.16	0.16
FeO	1.04	6.54	8.70	8.68
CaO	0.30	11.83	6.13	7.72
Na_2O	5.85	3.38	3.19	3.61
K_2O	1.78	1.07	3.05	1.56
P_2O_5	n.a.	0.81	0.97	0.81
SO_3	n.a.	0.86	0.97	0.83
Cl	n.a.	0.17	0.14	0.11
V_2O_5	n.a.	0.20	0.22	0.19
total	100.48	95.33	97.10	96.00

Discussion

Spinel substitutions

Although there is nearly complete solid solution between the magnetite-ulvöspinel spinels and the chromate and aluminate spinels at magmatic temperatures (Sack & Ghiorsio 1991), no continuous solid solution has been observed in studied samples. In Mesozoic alkali basalts both discrete phases (Cr-spinels and Fe-Ti spinels) are present. Cr-spinel (peridotitic and volcanic) compositional variations follow the effects of tetrahedral $Mg \leftrightarrow Fe^{2+}$ substitution (Fig. 8a) and octahedral $Cr \leftrightarrow Al$ substitution (Fig. 8b), whereas $2Fe^{3+} \leftrightarrow Fe^{2+}+Ti^{4+}$ exchange takes place in Fe-Ti spinels (magnetite–ulvöspinel series) (Fig. 8c). $Cr \leftrightarrow Al$ substitution is a dominant mechanism for Cr-spinel chemical variability. The described substitution trends are identical with those reported for Madeira Island alkaline lava (Mata & Munhá 2004).

Fe-Ti spinels from CWC alkalic rocks are somewhat poorer in Ti (Usp_{8-38}) than those from other alkali basalts occurrences (e.g. Usp_{52-71}, Corner & Maury 1980; Price & Taylor 1980, etc.). Ti-depletion of the studied Fe-Ti spinels could be explained in terms of alteration processes (Fig. 3f). Fe-Ti spinels in alkali basalts are richer in minor components (Al and Mg) than those from tholeiitic rocks and andesites. The distinctive feature of Fe-Ti spinels from alkalic rocks is their tendency toward high Al_2O_3 content (Frost & Lindsley 1991).

Cr-spinel alteration

Alteration processes were recognized on the basis of chemistry and textural changes (Fig. 3). Alteration processes mainly affected volcanic chromium spinels. In comparison to unaltered volcanic spinels, altered Cr-spinels typically have a higher TiO_2 content (up to 8.4 wt. %). Al_2O_3 contents are lower (17–24 wt. %), and so are Cr_2O_3 contents (12–20 wt. %) and MgO (usually between 8–12 wt. %, rarely ~3 wt. %). Altered spinels are enriched in FeO (15–26 wt. %) and Fe_2O_3 (15–35 wt. %). Two distinct trends of Al_2O_3 and Cr_2O_3 loss are displayed in Fig. 9. The Al/Cr loss ratios are rather similar (1.56–1.77 respectively, which means a Al/Cr loss rate of 3:2) and depend on the initial composition of unaltered Cr-spinels. The average Al_2O_3 and Cr_2O_3 loss in the first trend is 34.5 % and 22.2 % respectively. The second trend shows Al_2O_3 loss of 30.7% and Cr_2O_3 loss of 26.2 %. Generally, dissolution of MgO, Al_2O_3 and enrichment in FeO, Fe_2O_3 and TiO_2 were recognized. Changes (usually enrichment) in MnO, ZnO and V_2O_5 content are not so evident. Altered spinels have only a slightly higher content of these oxides.

Implication for the source of detrital spinel

We compared the composition of spinels from Cretaceous alkali volcanics with detrital spinels of volcanic origin from Cretaceous sedimentary rocks (Fig. 6, Table 3, Fig. 10). The most detrital volcanic spinels (following the discrimination criteria proposed by Lenaz et al. 2000; Kamenetsky et al. 2001) in CWC Cretaceous sediments were found in the Poruba flysch Formation (Albian) in the Tatric and Fatric (Krížna Nappe) Units. Some localities in the Poruba Flysch Formation show 37 % of volcanic spinels in the whole spinel population. Detrital volcanic spinels have a different composition

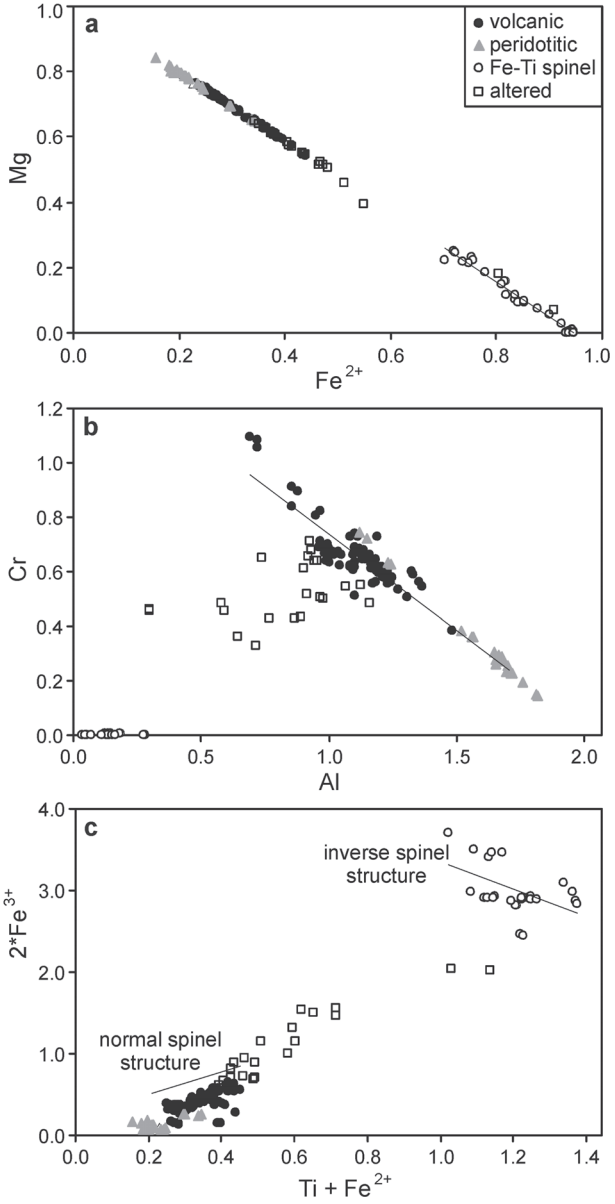

Fig. 8. Correlation of major elements in spinels from Mesozoic alkali basalts of Slovakia.

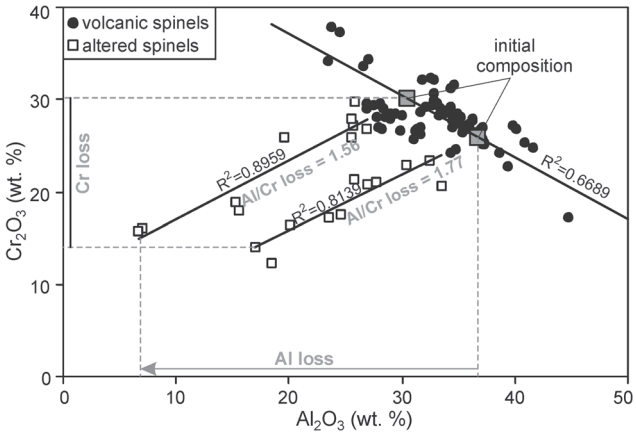

Fig. 9. Relationship between Al and Cr during alteration of spinels from Mesozoic alkali basalts of the Western Carpathians.

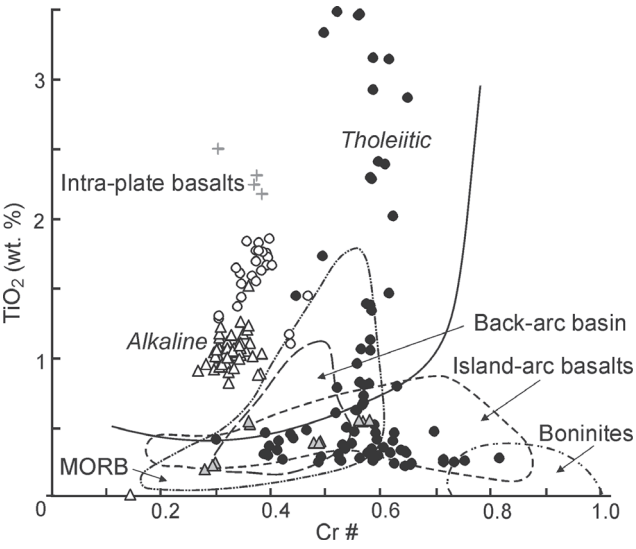

Fig. 10. Cr# vs. TiO_2 compositional relationship in volcanic Cr-spinels from the Mesozoic alkali volcanic rocks in comparison with detrital spinels from Cretaceous flysch sediments of the Western Carpathians (black circles). Compositional fields are after Arai (1992). Symbols as in Fig. 3.

(usually are richer in Cr_2O_3 and TiO_2) from those of alkali volcanic rocks and most of them correspond to the spinels from back-arc basin basalts (BABB) or mid-ocean ridge basalts (MORB) according to the classification by Kamenetsky et al. (2001). Volcanic spinels from Cretaceous alkali volcanics correspond to intra-plate alkali basalts (Fig. 10). Therefore, Mesozoic alkali rocks most probably could not be an important source of detrital spinel in Cretaceous sediments of the Tatric and Fatric Tectonic Units. Another argument for this suggestion could be knowledge that Fe-Ti spinels (titanomagnetites), which are quite usual on some alkali volcanic outcrops, were not found among detrital spinels. The source of detrital spinel in the Poruba Formation remains unknown.

One of the solutions for the source rock of detrital volcanic Cr-spinel from the Poruba Flysch Formation could be back-arc basin basalts (BABB) of the Meliata Ocean. The opening of the Meliata Ocean is in general interpreted as a result of back-arc rifting due to Paleotethys subduction under the Euroasian plate (e.g. Stampfli et al. 1998). The initial stages of the Meliata Ocean opening as a back-arc basin (with BABB) with later conversion to typical MORB is suggested by Ivan (2002).

The composition of peridotitic spinels from Mesozoic alkali volcanic rocks is similar to those of spinels from type I peridotites, according to Dick & Bullen (1984) and they show lherzolite character. In some cases (Podmanín) this type of spinel could be a part of disintegrated upper-mantle xenoliths, entrapped in magma of low viscosity.

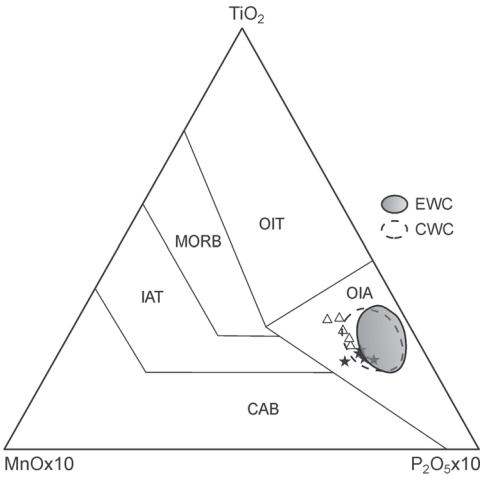

Fig. 11. Discrimination diagram of basalts according to Mullen (1983). **OIT** — ocean island tholeiites, **OIA** — ocean island alkaline basalts, **CAB** — volcanic arc calc-alkaline basalts, **IAT** — island arc tholeiites, **MORB** — mid-ocean ridge basalts. Fields of Cretaceous basalts from the EWC and CWC are after Hovorka & Spišiak (1988), Hovorka et al. (1999). Symbols as in Fig. 7.

Cr-diopside phenocrysts could be part of these upper-mantle xenoliths as well. However, there is one contradiction. The Cr-rich spinel inclusions from Cr-diopside correspond to the spinels from harzburgite. In this case, mantle rocks should represent both rock types.

Melt composition

Cpx inclusions associated with residual glass crystallized (1143–1183 °C and 0.50–0.68 GPa) within the host spinel from the entrapped melt as a phase in equilibrium with spinel (cpx + sp). The composition of the residual glass is slightly different from that of whole rock analyses reported from CWC by Hovorka & Spišiak (1988) and Hovorka et al. (1999) (Fig. 7). However, the composition of bulk melt (residual glass + daughter cpx + X % spinel) partly overlaps the field of Cretaceous basalts from the CWC. The alkali character of the melt is apparent from the TAS diagram. Tectonic affinity of the basaltic volcanites is shown in a discrimination diagram after Mullen (1983). Residual glass and bulk melt compositions are situated in the ocean island alkaline basalt field (Fig. 11). The bulk melt composition is the same as reported by Hovorka & Spišiak (1988) and Hovorka et al. (1999) from the CWC.

Cpx phenocryst

Three essential types of cpx phenocrysts were observed in alkali basalts from the CWC: (1) oscillatory zoned (Ti-rich) diopside phenocrysts, (2) Fe-rich diopside cores with oscillatory zoned Ti-rich rims and (3) Cr-diopsides. According to the Al^{VI}/Al^{IV} ratio, Na_2O, TiO_2 content and pyroxene barometry (Nimis 1995), high- and low-pressure cpx phenocrysts can be distinguished. In general, high-pressure cpx has a higher Al^{VI}/Al^{IV} ratio (> 1) along with a higher Fe/Fe + Mg ratio, higher Na_2O content and lower TiO_2 content (Dobosi & Horváth 1988). The Cr-diopsides and Fe-rich cores could be high-pressure phases (high Al^{VI}/Al^{IV} ratio, higher Na_2O content) originated in the upper mantle. Oscillatory zoned diopsides with higher TiO_2 content, low Na_2O content and low Al^{VI}/Al^{IV} ratio are supposed to be low-pressure cpx, which could crystallize in a crustal magmatic reservoir or during magma ascent.

Conclusions

- Volcanic spinels, peridotitic spinels and altered spinels were distinguished according to spinel chemical composition.
- Peridotitic spinels are supposed to originate in mantle peridotites and most likely represent relics of upper-mantle xenoliths, which had been entrained during the eruption of alkali volcanites.
- Mesozoic alkali volcanites were not a principal source for detrital Cr-spinels in Cretaceous flysch sediments.
- Cpx phenocryts reflect at least two stages of magma evolution (upper-mantle cpx → 1.34–1.48 GPa and Ti-rich zoned crustal cpx → 0.41–0.69 GPa).

Acknowledgments: We thank Dr. V. Hurai, Dr. D. Lenaz and an anonymous reviewer for critical reviews and constructive comments on a preliminary draft of this paper which greatly improved the final version. We are thankful to J. Spratt, A. Kearsley and Dr. T. Williams from the Natural History Museum in London for help with works on electron microprobe. This study also represents a partial output from the Grants APVT-51-012504, APVV-51-046105, VEGA 1/2031/05 and VEGA 2/6092/26.

References

Andersen D.J., Lindsley D.H. & Davidson P.M. 1995: QUILF — A program to assess equilibria among Fe-Mg-Ti oxides, pyroxenes, olivine, and quartz. *Computers in Geoscience* 19, 1333–1350.

Arai S. 1992: Chemistry of chromian spinel in volcanic rocks as a potential guide to magma chemistry. *Mineral. Mag.* 56, 173–184.

Bujnovský A., Kantor J. & Vozár J. 1981: Radiometric dating of Mesozoic basic eruptive rocks of the Krížna nappe in the NW part of the Low Tatra. *Geol. Zbor. Geol. Carpath.* 32, 221–230.

Corner G. & Maury R.C. 1980: Petrology of the volcanic island of Annobon, Gulf of Guinea. *Mar. Geol.* 36, 253–267.

Deer W.A., Howie R.A. & Zussman J. 1992: An introduction to the rock-forming minerals (2nd Edition). *Longman*, England, 1–696.

Dick H.J.B. & Bullen T. 1984: Chromian spinel as a petrogenetic indicator in abyssal and alpine-type peridotites and spatially associated lavas. *Contr. Mineral. Petrology* 86, 54–76.

Dobosi G. & Horváth I. 1988: High- and low pressure cognate clinopyroxenes from alkali lamprophyres of the Velence and Buda Mountains, Hungary. *Neu. Jb. Mineral. Abh.* 158, 3, 241–256.

Frost B.R. & Lindsley D.H. 1991: Occurrence of iron-titanium oxides in igneous rocks. In: Lindsley D.H. (Ed.): Oxide minerals: petrologic and magnetic significance. *Rev. Mineral.* 25, 433–462.

Hovorka D. & Spišiak J. 1988: Mesozoic volcanism of the Western Carpathians. *Veda,* Bratislava, 1–263.

Hovorka D., Dostal J. & Spišiak J. 1999: Geochemistry of the Cretaceous alkali basaltic rock of the central part of the Western Carpathians (Slovakia). *Krystalinikum* 25, 37–48.

Ivan P. 2002: Relics of the Meliata ocean crust: Geodynamic implications of mineralogical, petrological and geochemical proxies. *Geol. Carpath*ica 53, 245–256.

Irvine T.N. & Baragar W.R.A. 1971: A guide to the chemical classification of the common volcanic rocks. *Canad. J. Earth Sci.* 8, 523–548.

Jablonský J., Sýkora M. & Aubrecht R. 2001: Detritic Cr-spinels in Mesozoic sedimentary rocks of the Western Carpathians (overview of the latest knowledge). *Miner. Slovaca* 33, 487–498 (in Slovak).

Kamenetsky V.S., Crawford A.J. & Meffre S. 2001: Factors controlling chemistry of magmatic spinel: an empirical study of associated olivine, Cr-spinel and melt inclusion from primitive rocks. *J. Petrology* 42, 655–671.

Le Maitre R.W., Bateman P., Dudek A., Keller J., Le Bas M.J., Sabine P.A., Schmid R., Sorensen H., Streckeisen A., Woolley A.R. & Zanettin B. 1989: A classification of igneous rocks and glossary of terms. *Blackwell,* Oxford.

Lefeld J. 1985: Jurassic and Cretaceous lithostrafic units of the Tatra Mts. *Stud. Geol. Pol.* 84, 1–93.

Lenaz D., Kamenetsky V.S., Crawford A.J. & Princivalle F. 2000: Melt inclusion in detrital spinel from the SE Alps (Italy-Slovenia): a new approach to provenance studies of sedimentary basins. *Contr. Mineral. Petrology* 139, 748–758.

MacDonald G.A. & Katsura T. 1964: Chemical composition of Hawaiian lavas. *J. Petrology* 5, 1, 82–133.

Mata J. & Munhá J. 2004: Madeira Island alkaline lava spinels: petrogenetic implications. *Miner. Petrology* 81, 85–111.

Mello J. (Ed.), Potfaj M., Teťák F., Havrila M., Rakús M., Buček S., Filo I., Nagy A., Salaj J., Maglay J., Pristaš J. & Fordinál K. 2005: Geological map of the Middle Váh valley region 1:50,000. *ŠGÚDŠ,* Bratislava.

Mercier J-C.C. 1976: Single-pyroxene geothermometry and geobarometry. *Amer. Mineralogist* 603–615.

Mišík M., Jablonský J., Fejdi P. & Sýkora M. 1980: Chromian and ferrian spinels from Cretaceous sediments of the West Carpathians. *Miner. Slovaca* 42, 2, 101–112 (in Slovak).

Morimoto N. 1989: Nomenclature of pyroxenes. Subcomitee on pyroxenes. Commision on new minerals and mineral names. *Canad. Mineralogist* 27, 143–156.

Mullen E.D. 1983: $MnO/TiO_2/P_2O_5$: a minor element discriminant for basaltic rocks of oceanic environments and its implications for petrogenesis. *Earth Planet. Sci. Lett.* 62, 53–62.

Nimis P. 1995: A clinopyroxene geobarometer for basaltic systems based on crystal structure modeling. *Contr. Mineral. Petrology* 121, 115–125.

Papike J.J., Cameron K.L. & Baldwin K. 1974: Amphiboles and pyroxenes: Characterization at other than quadrilateral components and estimates of ferric iron from microprobe data. *Geol. Soc. Amer., Abstracts with Programs* 6, 1053–1054.

Plašienka D. 1999: Tectonochronology and paleotectonic model of the Jurassic–Cretaceous evolution of the Central Western Carpathians. *Veda,* Bratislava, 1–125.

Price R.C. & Taylor S.R. 1980: Petrology and geochemistry of the Banks Peninsula volcanos, South Island, New Zeland. *Contr. Mineral. Petrology* 72, 1–8.

Ryburn R.J., Raheim A. & Green D.H. 1976: Determination of P, T paths of natural eclogites during metamorphism — record of subduction. A correction to a paper by Rahaim & Green (1975). *Lithos* 9, 161–164.

Sack R.O. & Ghiorso M.S. 1991: Chromite as a petrogenetic indicator. In: Lindsley D.H. (Ed.): Oxide minerals: petrologic and magnetic significance. *Rev. Mineral.* 25, 323–353.

Spišiak J. & Hovorka D. 1997: Petrology of the Western Carpathians Cretaceous primitive alkaline volcanics. *Geol. Carpathica* 48, 2, 113–121.

Spišiak J. & Balogh K. 2002: Mesozoic alkali lamprophyres from granitoids from Malé Karpaty and Nízke Tatry Mts.- geochemistry and geochronology. *Geol. Carpathica* 53, 5, 283–294.

Stampfli G.M., Mosar J., Marquer D., Marchant R., Baudin T. & Borel G. 1998: Subduction and obduction processes in the Swiss Alps. *Tectonophysics* 296, 159–204.